Available online at www.sciencedirect.com
SCIENCE DIRECT
Polymer 47 (2006) 6208–6217
polymer
www.elsevier.com/locate/polymer

Formation and properties of nylon-6 and nylon-6/montmorillonite composite nanofibers

Lei Li [a], Leon M. Bellan [b], Harold G. Craighead [b], Margaret W. Frey [a,*]

[a] *Fiber Science and Apparel Design, Cornell University, 299 MVR Hall, Ithaca, NY 14853-4401, USA*
[b] *School of Applied and Engineering Physics, Cornell University, Ithaca, NY 14853-3501, USA*

Received 11 May 2006; received in revised form 20 June 2006; accepted 20 June 2006
Available online 11 July 2006

Abstract

Nanocomposite fibers of nylon-6 and an organically modified montmorillonite (O-MMT), Cloisite-30B, were prepared by electrospinning. Dispersion and exfoliation of O-MMT in nylon-6 were achieved by melt-extrusion in a twin-screw extruder prior to dissolving in aqueous formic acid for electrospinning. The effects of O-MMT layers on the properties of the nylon-6 solution and electrospun nanocomposite fibers were investigated. Homogeneous, cylindrical nanocomposite fibers with diameters ranging from 70 to 140 nm could be prepared from the 15% composite solution. The O-MMT layers were well exfoliated inside the nanocomposite fibers and were oriented along the fiber direction. Both the degree of nylon-6 crystallinity and the crystallite sizes increased for the nanocomposite fibrous mats, most significantly for those composed of the smallest fibers electrospun from 15% solution. The mechanical properties of the electrospun fibrous mats and single fibers depended not only on the addition of O-MMT layers but also on the sizes of the fibers. Smaller fibers exhibited higher Young's modulus.

Keywords: Electrospinning; Nanocomposite; Nanoclay

1. Introduction

Polymer/layered silicate nanocomposites (PLSNs) have attracted much attention in the last decade due to their increased modulus and strength and improved thermal and barrier properties [1,2]. Because of the nanometer size and high surface area of silicate layers, the significantly improved properties of PLSNs can be achieved with the silicate content lower than 5% when the silicate layers are homogeneously exfoliated in the polymer matrix [3,4]. The exfoliation of silicate layers is usually attained by in situ polymerization [5] or by polymer melt-extrusion [2]. The extrusion method has been shown to be more efficient and environmentally benign [3]. The exfoliation of silicate layers in a polymer matrix can also be improved by modifying the surface of pristine silicate layers with organic cations, such as alkylammonium, which renders the normally hydrophilic silicate surface organophilic [1].

The majority of research on PLSNs has focused on the molded bulk materials [1,2,5–7] with very few studies being reported more recently on the formation of PLSN fibers by electrospinning [8–12]. Since the mechanical properties of fibers in general improve substantially with decreasing fiber diameter, there is considerable interest in the development of continuous electrospun polymer nanofibers [13]. Lincoln et al. reported that the degree of crystallinity of nylon-6 annealed at 205 °C increased substantially with the addition of MMT, implying that the silicate layers could act as nucleating agents and/or growth accelerators [5]. In contrast, the study of Fong et al. showed a very similar overall degree of crystallinity for electrospun nylon-6 and nylon-6/Cloisite-30B nanocomposite fibers containing 7.5 wt% of O-MMT layers [8]. Fornes and Paul have found that O-MMT layers could serve as nucleating agents at low concentration, 3%, in nylon-6/O-MMT nanocomposite but retarded the crystallization of nylon-6 at high concentration

* Corresponding author. Tel.: +1 607 255 1937; fax: +1 607 255 1093.
E-mail address: mfw24@cornell.edu (M.W. Frey).

0032-3861/$ - see front matter © 2006 Elsevier Ltd. All rights reserved.
doi:10.1016/j.polymer.2006.06.049

around 7% [6]. In addition, the differences in the molecular weight of nylon-6 and the solvent used for electrospinning are also expected to have different impacts on the mobility of nylon-6 molecular chains and the interactions between the nylon-6 chains and O-MMT layers, which may also affect the crystallization behavior of nylon-6 molecules during the electrospinning.

In the electrospinning process, a high voltage is applied to the droplets of polymer solutions or melts to overcome the liquid surface tension and enable the formation of fibers with an average diameter in the sub-micron range [14,15]. Due to their small fiber diameter, high surface-to-volume ratio and controllable porous structures, electrospun fibrous mats have been studied for a variety of applications such as filter media [16,17], footwear and clothing [18], reinforcement materials [19], smart hydrogel fibers [20] and tissue engineering [21]. For most practical applications, strong polymer nanofibers are desired. In order to improve the mechanical properties of electrospun polymer fibers, nanoparticles such as layered silicates [9,11,12] and carbon nanotubes (CNT) [22,23] have been incorporated to form nanocomposite fibers. Since the mechanical properties of the electrospun fibrous mats are determined by not only the properties of individual fibers but also by the distribution and orientation of the fibers in the mats [24], it is of fundamental interest to investigate the mechanical properties of both electrospun fibrous mats and a single electrospun fiber.

Although the mechanical properties of electrospun fibrous mats can be easily measured using a tensile tester [12,24], very few techniques have been developed to investigate the mechanical properties of individual electrospun fibers due to their small diameters. Kim et al. investigated the deformation behavior of poly(methyl methacrylate) (PMMA)/Na-montmorillonite (Na-MMT) nanocomposite electrospun fibers by observing an in situ stretched single fiber under TEM [25]. While the bulk nanocomposite deforms in a brittle manner, the nanocomposite electrospun fiber deforms by shear yielding in the form of necking that resulted from the ultra-highly nanoporous structures on the fiber surface due to the presence of the nanoclay [25]. Ji et al. characterized the surface nanomechanical properties of electrospun polystyrene (PS) fibers by shear modulation force microscopy (SMFM) and found that the relative surface modulus of electrospun PS single fibers increased with the decreasing fiber sizes [11]. Very recently, atomic force microscopy (AFM) has been utilized to characterize the mechanical properties of individual electrospun fibers. Wang et al. determined the Young's modulus of individual electrospun silk fibers by nanoindentation [26] and observed an increase in the Young's modulus with increasing degree of crystallinity of silk fibers. Bellan et al. derived the Young's modulus of single electrospun poly(ethylene oxide) (PEO) fibers from the force–displacement curves obtained by depressing the individual fibers with an AFM probe [27] and the same method was utilized in this paper. The basis of the technique is the measurement of the deflection of an electrospun nanofiber by application of a known load using an AFM probe. The Young's modulus of the fiber can be calculated from the displacement of the fiber under the load together with the dimension of the tested fiber. Tensile test is another widely used method for measuring the Young's modulus of fibers, which involves measuring the load–elongation behavior of the fiber with known cross-sectional area [28]. The Young's moduli of SiC–fiber-reinforced DURAN glass composites obtained from conventional three-point testing and tensile test methods were shown to be in good agreement [29]. However, since the diameter of the electrospun nylon-6/O-MMT fibers is only about a few hundred nanometers, it is impossible to grip a single fiber between the clamps of a conventional tensile tester to measure the Young's modulus.

Since very few studies have been performed on PLSN nanofibers, more research needs to be conducted in this area in order to better understand the formation and properties of PLSN nanofibers. In this study, the nylon-6/organically modified montmorillonite (O-MMT) nanocomposite prepared by melt-extrusion was dissolved in aqueous formic acid and electrospun into nanofibers. Although the solvent may form hydrogen bonding and have electrostatic interactions with O-MMT layers, no phase separation was observed between nylon-6 and O-MMT layers. The exfoliation of O-MMT layers in the melt-extruded nanocomposite was well preserved in the electrospun fibers. Meanwhile, the effects of O-MMT on the mechanical properties of electrospun nylon-6 fibrous mats and individual fibers were investigated and compared. The enhanced Young's modulus and ultimate tensile strength were observed for nylon-6/O-MMT nanocomposite fibrous mats when compared with nylon-6 electrospun fibrous mats with similar fiber sizes. However, our results also showed that the electrospun nanocomposite fibrous mats would have a lower tensile strength than pure nylon-6 fibrous mats if the nanocomposite fibers were much larger. In other words, in order to achieve improved mechanical properties for electrospun nylon-6/O-MMT nanocomposite fibrous mats, the fiber size has to be taken into account, which is not a concern for bulk nanocomposite materials. In addition, the Young's moduli of individual nanocomposite fibers and nylon-6 fibers increased with decreasing fiber sizes and were significantly higher for nanocomposite fibers at the similar fiber diameters. To the best of our knowledge this is the first time characterization of the mechanical properties of the electrospun nylon-6 and nylon-6/O-MMT nanocomposite fibrous mats and individual fibers has been compared.

2. Experimental

2.1. Materials

Organically modified montmorillonite (O-MMT), Cloisite-30B, purchased from Southern Clay Products Inc. is a natural montmorillonite modified with a quaternary ammonium ion, $N^+(CH_2CH_2OH)_2(CH_3)T$, where T represents tallow (~65% C_{18}, ~30% C_{16}, and ~5% C_{14}). The cation exchange capacity of Cloisite-30B is 90 meq/100 g of clay. The dry particle size distribution of Cloisite-30B is 10% less than 2 μm, 50% less than 6 μm and 90% less than 13 μm. Each Cloisite-30B dry particle, however, may contain several thousands or even many more individual platelets, which may be well exfoliated, intercalated or aggregated in the PLSNs depending on the

interactions between polymers and O-MMT and the processing techniques used to prepare the PLSNs [30]. Nylon-6 ($M_w = \sim 10{,}000$ Da) and 88% formic acid were purchased from Aldrich and VWR International, respectively. All materials were used as received.

2.2. Preparation and electrospinning

Nylon-6/O-MMT composite with 5 wt% of O-MMT, designated as NC5, was prepared by blending nylon-6 and Cloisite-30B using a twin-screw extruder operating at 250 °C and 110 rpm for 3 min under N_2 protection. Both nylon-6 and Cloisite-30B were dried at 80 °C for 24 h under vacuum before the blending and extrusion.

Uniform nylon-6 and NC5 solutions were prepared in 88% formic acid at room temperature by gently stirring for 8 h. All solution concentrations are expressed as weight percentages.

The electrospinning was performed using a single syringe attached to a 24 gauge needle (Hamilton 90024, VWR Inc.). The solution was fed at a rate of 0.1 ml/h using a syringe pump (Model 100 kdScientific) and the tip-to-collector distance was 14 cm. A high voltage power supply (Gamma High Voltage Supply, ES 30−0.1P) was connected to the syringe needle. The electrospinning voltage was about 29 kV. A piece of aluminum foil was grounded and used as the collector unless stated differently.

2.3. Measurement and characterization

The zero-shear-rate solution viscosity was measured using a Rheometrics AR 2000 rheometer. The solution conductivity and surface tension were determined with a conductivity meter (VWR International) and a wetting balance (Cahn D200, TRI), respectively.

The morphology of the electrospun fibers was observed with a scanning electron microscope (SEM, LEICA 440). The fibers were coated with gold and observed under 25 kV accelerating voltage. About 100 electrospun fibers were measured using image analysis software (Scion Image, NIH Image software) to obtain the fiber size distribution. Transmission electron microscope (TEM) images of fibers were obtained using an LEO 922 energy filtered TEM (EFTEM) operating at 200 kV. Thin cross sections of fibers were prepared in order to observe the distribution of silicate layers within the nanocomposite fibers. The fibers were embedded in epoxy and sectioned at approximately 70 nm thickness using a microtome (Sorvall Ultra Microtome, MT 5000, DuPont) equipped with a diamond knife at room temperature. The sections were then stained with osmium tetroxide for 1 h and imaged using a JEOL 1200EX TEM operating at 120 kV. Amorphous nylon-6 film was prepared by melting nylon-6 pellets at 250 °C for about 5 min and quenching in liquid nitrogen. Wide angle X-ray diffraction (WAXD) was conducted using a Scintag PADX diffractomer using an incident X-ray wavelength of 1.542 Å at a step rate of 0.02° and at a scan rate of 1.0°/min. The resulting plots of X-ray intensity versus 2θ were analyzed by the profile-fitting program DMSNT ThermoARL. Areas of the peaks obtained from the analysis were used to estimate the degree of crystallinity for each phase, i.e., the ratio of the areas of the crystalline reflections to that of the total area of the crystalline and amorphous phases. The thermal behavior of nylon-6 and NC5 electrospun membranes was determined with a differential scanning calorimeter (DSC) (DSC 2920, TA Instruments Inc.) using ~5.0 mg samples at a 10 °C/min heating rate in nitrogen. The degree of crystallinity was calculated by subtracting the measured heat of cold crystallization from the measured heat of fusion and dividing by the heat of fusion of the purely crystalline forms of nylon-6. To determine the exact amount of O-MMT in the final electrospun nylon-6/O-MMT nanocomposite fibers, about 20 mg of previously dried nanocomposite fibers were heated at 900 °C for 45 min in the furnace of a thermogravimetric analyzer (TGA) (TGA 2050, TA Instruments Inc.). The percent O-MMT in the nanocomposite fibers (%O-MMT) was calculated from the following equation:

$$\%\text{O-MMT} = \%\text{O-MMT}_{\text{ash}}/0.935$$

where $\%\text{O-MMT}_{\text{ash}}$ is the mass after incineration relative to the original nanocomposite mass. The quantity 0.935 in the equation accounts for the loss of structural water during incineration [31]. The calculated result showed that there was about 4.1 wt% O-MMT in the nylon-6/O-MMT nanocomposite fibers.

The tensile properties of the electrospun nanofibrous mats were measured using an Instron tensile tester (Instron 5566) equipped with a 100 N load-cell at 65% RH and 23 °C. The size of the electrospun mats was 50 mm in length and 10 mm in width. The thickness of the mats was about 0.03 mm, measured using a micrometer. The gauge length was 30 mm and the cross-head speed was 5 mm/min. The reported Young's modulus, ultimate strength and ultimate strain for the electrospun nanofibrous mats were the average of three to six tests.

The Young's modulus of suspended nylon-6 and NC5 electrospun nanofibers was determined by depressing the single fibers with an atomic force microscope (AFM) probe (Dimension 3000, Digital Instruments) using the procedure that has been previously described [27]. Instead of collecting the electrospun fibers on a piece of static Al foil, electrospun NC5 and nylon-6 fibers, in this case, were deposited on a silicon chip in which several trenches had been etched. The trenches were 10−80 μm wide and 5−10 μm deep. The silicon chip was put on a rotating plate, which allowed us to orient the fibers relative to the trenches. The electrospinning was conducted for only a few seconds to prevent overlapping of fibers. Single fibers, which were fully suspended and not in contact with other fibers over the trench, were used for the measurements.

3. Results and discussion

3.1. Fiber morphology

Both nylon-6 and NC5 were readily soluble in 88% aqueous formic acid. O-MMT did not precipitate from the NC5 solutions even after solutions were stored for several days. The

Table 1
Solution properties and electrospun fiber diameter

Sample	Concentration (wt%)	Viscosity (Pa s)	Conductivity (mS/cm)	Surface tension (mN/m)	Fiber size (nm)
Nylon-6	15	0.5	4.62	41.21	–
	20	1.5	4.30	42.33	120
NC5	15	0.8	4.91	41.28	95
	20	2.4	4.70	41.54	400

zero-shear-rate solution viscosity increased with increasing concentration for both nylon-6 and NC5 solutions (Table 1). The NC5 solutions exhibited a 60% higher viscosity than the nylon-6 solutions at the same solution concentration. On the other hand, the solutions exhibited a lower conductivity at higher concentrations for both the types of solutions. No obvious dependence of solution surface tension on concentration was observed. Since lower solution viscosity and higher solution conductivity favor thinner fibers, the average fiber size increase with increasing solution concentration was expected (Table 1). SEM images of samples electrospun from the 15% nylon-6 solution showed not only fibers but also many bead structures (Fig. 1a). However, very homogeneous fibers without bead-on-string structures were electrospun from the NC5 solution at the same concentration (Fig. 2a). The average fiber diameter was approximately 100 nm (Fig. 2b). The improved fiber uniformity is attributed to the higher viscosity and conductivity of the 15% NC5 solution when compared with 15% nylon-6 solution. Based on the fiber size distribution of 100 fibers (Fig. 1c) from several SEM images with one example shown in Fig. 1b, about 85% of fibers had diameters between 100 and 180 nm and 11% of fibers larger than 300 nm. Meanwhile, some flat-sheet or ribbon-shaped fibers with diameters as large as 1 μm were observed (Fig. 1b). Fibers with flat-sheet shape were also produced when electrospun from 20% NC5 solutions (Fig. 2c). Some flat-sheet fibers were twisted as indicated by the arrows in the images, which made them easy to observe (Fig. 2c). Fong et al. [8] reported ribbon-shaped nylon-6 fibers during electrospinning of nylon-6/hexafluoroisopropanol (HFIP) solution and speculated that rapid solvent removal from the surface of the jet presumably forms a skin, reducing subsequent solvent evaporation. This skin may cause the formation of hollow tubes, which subsequently collapse to form ribbons. Ribbon-shaped electrospun fibers and branched fibers have been reported from a number of different kinds of polymers and solvents [32]. We did not observe the flat-sheet shaped fibers, however, in samples electrospun from 15% nylon-6 or NC5 solution. The lower solution viscosity and higher conductivity of 15% solution correspond to increased draw down and whipping of the fiber close to the spinneret before the formation of a skin layer resulting from the solvent evaporation from the solution jet could occur. Meanwhile, 88% aqueous formic acid has a much higher boiling point (bp = 101 °C) than HFIP (bp = 59 °C), which will also decrease the opportunity for the formation of flat-sheet or ribbon-shaped fibers.

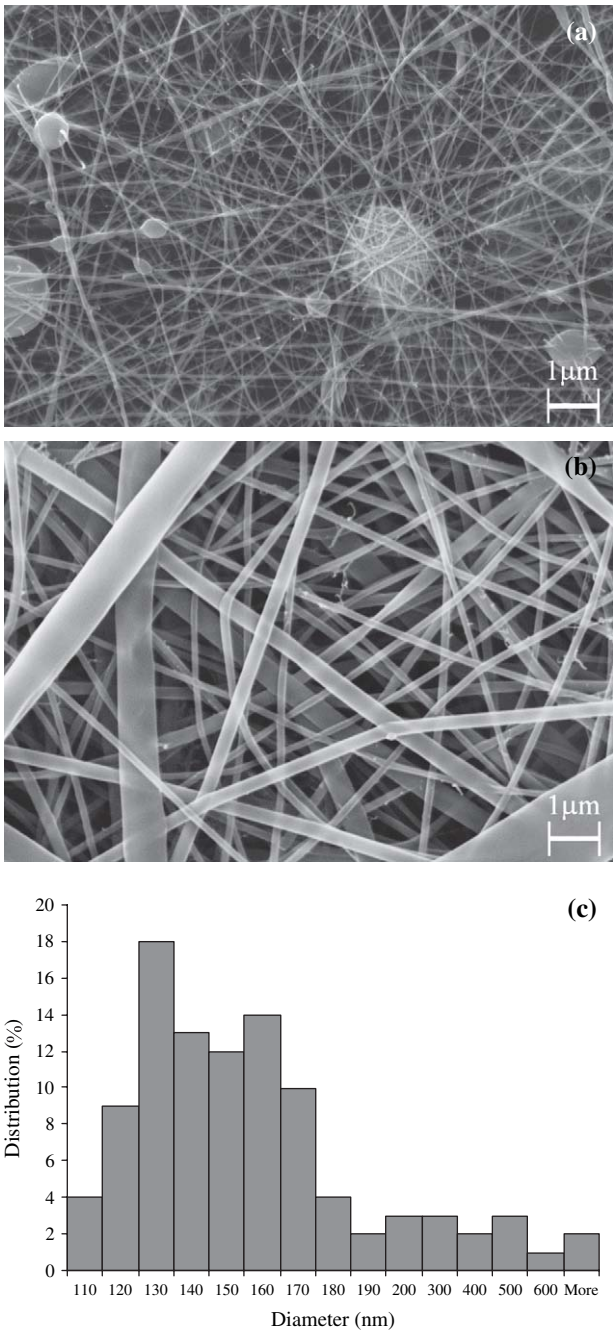

Fig. 1. SEM images of nylon-6 fibers electrospun from (a) 15% and (b) 20% solutions. The size distribution of nylon-6 fibers electrospun from 20% solution was shown in (c).

3.2. Distribution of O-MMT layers in electrospun NC5 nanocomposite fibers

The distribution of O-MMT layers in the NC5 nanocomposite fibers was investigated by bright field TEM imaging. Fig. 3 shows typical TEM images of composite fibers electrospun from 15% NC5 (Fig. 3a) and 20% NC5 (Fig. 3b) solutions. The O-MMT layers, dark lines in the TEM images, are about 1 nm thick, indicating complete exfoliation of O-MMT layers. All O-MMT layers are oriented in the fiber axial direction. This orientation confirms that extensional forces are exerted

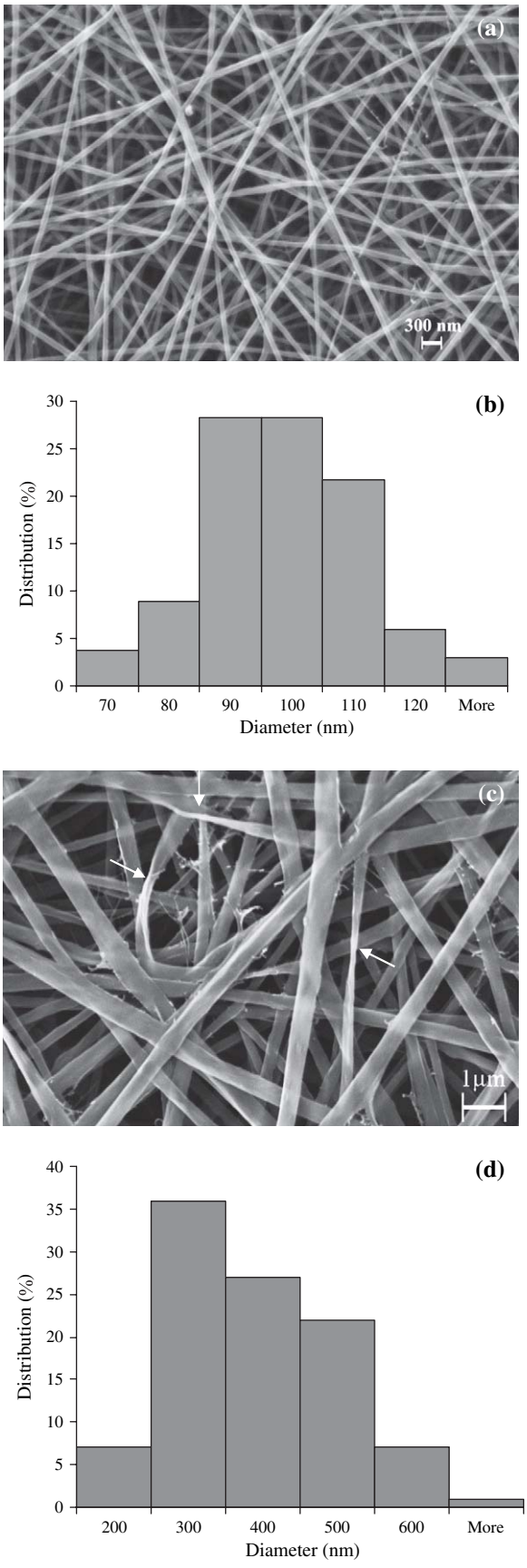

Fig. 2. SEM images of nylon-6/O-MMT nanocomposite fibers electrospun from (a) 15% and (c) 20% NC5 solutions with corresponding fiber size distribution shown in (b) and (d), respectively. The magnification bar is 300 nm in (a) and 1 μm in (c). The arrows in (c) indicate the twisting part of the flat-sheet fibers.

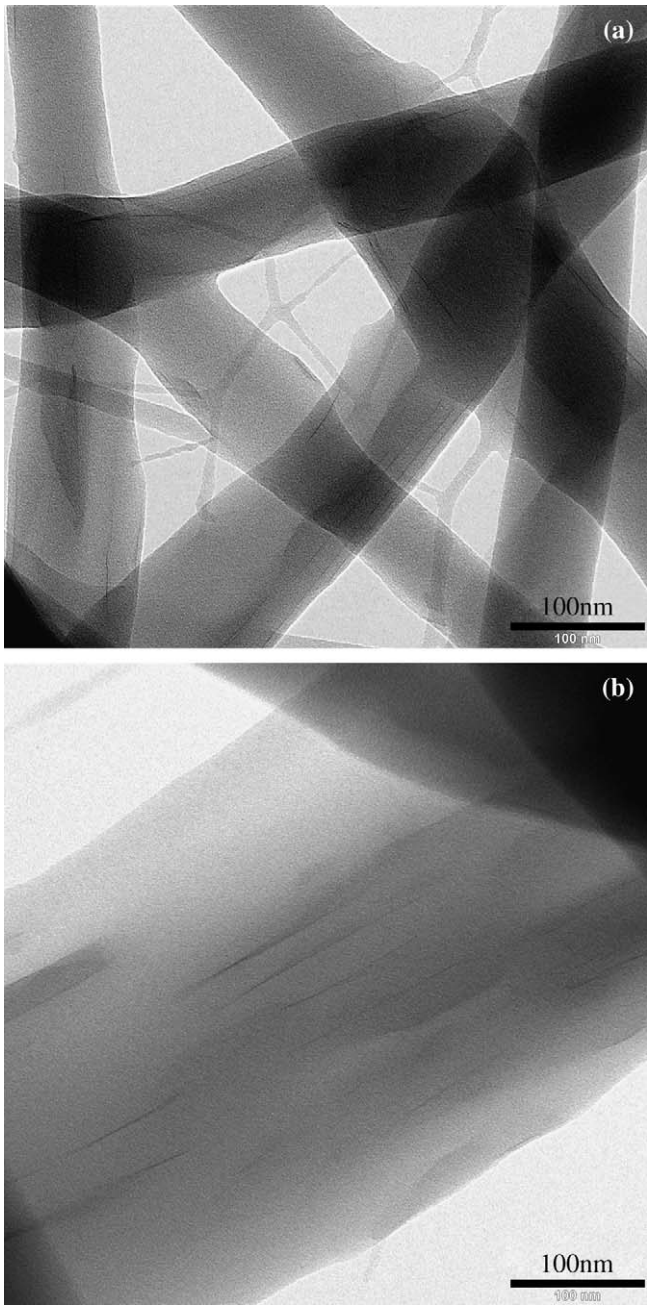

Fig. 3. TEM images of nylon-6/O-MMT nanocomposite fibers electrospun from (a) 15% and (b) 20% NC5 solutions.

on the fibers during electrospinning. Nanofibrils with diameters below 10 nm were observed between the larger primary nanofibers in samples electrospun from 15% NC5 solution (Fig. 3a). Existence of nanofibrils can be attributed to the branching of primary nanofibers during the electrospinning [32]. The O-MMT layers existed in the primary nanofibers only. The dimensions of the branched nanofibrils were too small to hold the O-MMT layers. The lower viscosity of 15% NC5 solution seemed to favor the formation of nanofibrils since significantly fewer

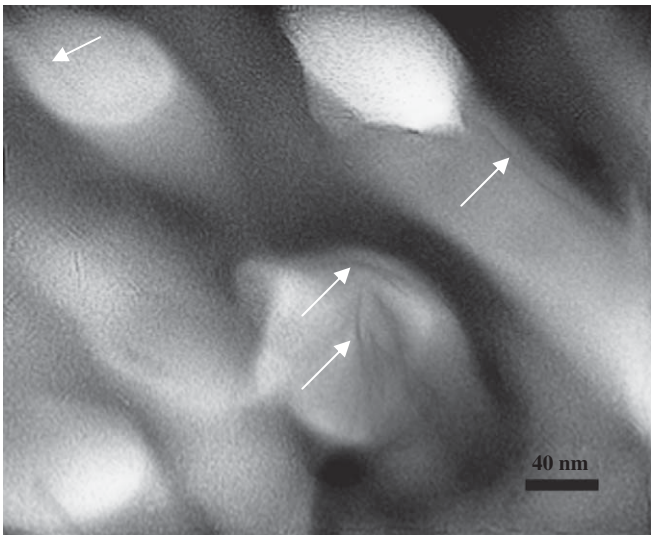

Fig. 4. TEM image of ultra-thin sections of nylon-6/O-MMT nanocomposite fibers electrospun from 15% NC5 solution. The arrows in the image indicate the O-MMT layers.

nanofibrils are observed from the electrospinning of 20% NC5 solutions.

The TEM images of ultra-thin nanocomposite fiber sections confirmed that the O-MMT layers were well exfoliated inside the fibers (Fig. 4). Since the fiber sections were only about 100 nm in diameter and 70 nm in thickness, O-MMT layers were not observed in all fiber sections. Depending on the cutting planes on the fibers, fiber sections exhibited either round or elliptical shapes. Some fibers were cut in the direction parallel to the fiber axis and as a result a longitudinal section was observed. Some O-MMT layers appeared as very thin and straight dark lines inside the fibers and some were observed as bent or curved thin lines. The bent O-MMT layers sometimes exhibited curvatures similar to the fiber cross-sections, suggesting that the O-MMT layers could be bent during the fiber formation process.

It is worth noting that the solvent used in this research, 88% aqueous formic acid, can form hydrogen bonds with the hydroxyl groups on the surfaces of O-MMT layers. Electrostatic interaction may also occur between the charged O-MMT surfaces and formic acid molecules since formic acid can dissociate in the aqueous environment. However, the hydrogen bonding and electrostatic interactions between O-MMT layers and the solvent did not cause phase separation between nylon-6 molecules and O-MMT layers in the solution or re-agglomeration of the O-MMT. The exfoliation of O-MMT layers in the nylon-6 matrix formed during the melt compounding process was well conserved in the electrospun nanocomposite fibers. Similar observation on the exfoliation of O-MMT layers has been made by Fong et al. when the nylon-6/O-MMT fibers were electrospun from solutions of melt-extruded composite pellets in HFIP [8]. However, O-MMT layers collapsed and yielded intercalated O-MMT aggregates in composite fibers electrospun from the HFIP/dimethyl-formamide (DMF) co-solvent [8]. Aggregation of O-MMT was attributed to the hydrogen bonding between DMF and O-MMT, effectively leading to phase separation between O-MMT and nylon-6.

3.3. X-ray diffraction and thermal analysis of NC5 nanocomposite fibers

Since the number of fibers that could be observed by TEM images was small, the distribution of O-MMT layers in the NC5 electrospun nanocomposite fibers was further investigated by wide angle X-ray diffraction (WAXD). Fig. 5 shows the WAXD patterns of amorphous nylon-6 film, electrospun nylon-6 fibers, NC5 nanocomposite fibers and the O-MMT (Cloisite-30B). Amorphous nylon-6 film showed a broad diffraction peak at $2\theta = 21.3°$. WAXD profiles confirmed that electrospun nylon-6 and NC5 nanocomposite fibrous mats also contained amorphous nylon-6. The electrospun nylon-6 and NC5 composite fibers exhibited strong peaks at $2\theta = 8.6°$ and 17.2°, and two weak diffraction peaks at $2\theta = 25.8°$ and 28.5° in addition to the amorphous peak. Peak at $2\theta = 8.6°$ is characteristic of the α phase of nylon-6 crystallite and the one at 17.2° of the γ phase crystallite [5]. A diffraction peak at $2\theta = 28.5°$ was also reported for nylon-6 crystallized at 180 °C and nylon-6/montmorillonite nanocomposite crystallized between 0 °C and 180 °C by Zhao et al., but no crystal structure and reflection plane have been assigned to this peak [33]. The O-MMT showed a diffraction peak at 4.8° corresponding to a *d*-spacing of 1.85 nm (inset in Fig. 5), which was, however, not observed for the electrospun NC5 nanocomposite fibers. The absence of O-MMT peak from the WAXD patterns of NC5 nanocomposite fibers confirmed that the O-MMT layers were well exfoliated in the fibers [7].

The degree of crystallinity of the electrospun nylon-6 and NC5 nanocomposite fibers is summarized in Table 2. The addition of O-MMT caused an increase in the degree of crystallinity for all crystalline phases of nylon-6. The orientation of O-MMT layers as shown by the TEM images (Fig. 3) may help to improve the orientation of nylon-6 molecules in the composite fibers due to the affinity between O-MMT layers and nylon-6 molecules thus facilitating crystallization. The O-MMT layers may also serve as a nucleating agent to

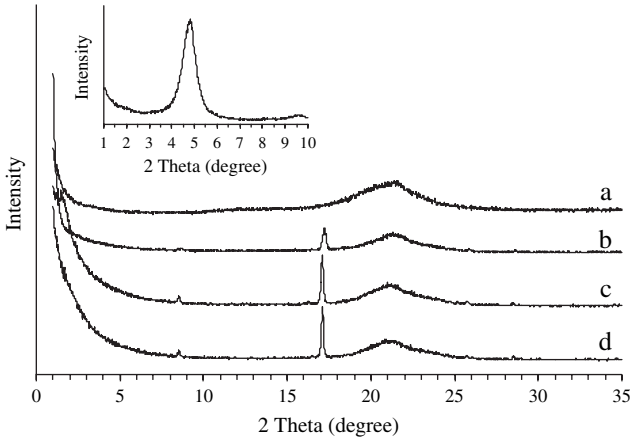

Fig. 5. WAXD patterns of (a) amorphous nylon-6; and fibers electrospun from (b) nylon-6; (c) 20% NC5 and (d) 15% NC5 nanocomposite solutions. The inset is the WAXD pattern of O-MMT, Cloisite-30B.

Table 2
Degree of crystallinity obtained from wide angle X-ray diffraction patterns of electrospun nylon-6 and NC5 membranes

Sample	%α	%γ	%Unknown	Total (%)	Size of α-form of nylon-6 crystal (nm)
Nylon-6	6.4	1.2	0.6	8.2	49.7
15% NC5	10.5	1.5	1.0	13.0	58.1
20% NC5	8.8	1.2	0.8	10.8	57.2

facilitate the nylon-6 crystallization especially when the O-MMT layers are well exfoliated [5,6]. Lower concentration solutions for electrospinning had lower viscosity, higher conductivity and greater solvent content than higher concentration solutions. These factors combine to increase both the extensional forces acting to draw down the fiber and the length of time the solvent remained in the fiber, and thus can facilitate nylon-6 chain mobility. It was not surprising to find that samples electrospun from 15% NC5 solutions had higher crystallinity than samples electrospun from 20% NC5 solutions.

The size of nylon-6 crystals in the electrospun nylon-6 and NC5 fibers was determined by measuring the full width of the WAXD peak at half maximum (FWHM) and comparing it with an Alumina (Al_2O_3) standard (NIST 1976). The crystallite sizes of α-form nylon-6 crystals determined from the FWHM of the WAXD peak at 17.6° were 49.7, 58.1 and 57.2 nm for electrospun nylon-6, and NC5 nanocomposite fibers electrospun from 15% and 20% solutions, respectively (Table 2). The crystallite sizes were comparable to the fiber sizes and were almost half of the average diameter of NC5 fibers and nanocomposite fibers electrospun from 15% solution. Similar observation has been made by Lincoln et al. on the increased crystallite size of nylon-6 during the isothermal crystallization with the addition of MMT [5].

The crystallization behavior of electrospun nylon-6 and NC5 fibers was also investigated using a differential scanning calorimeter (DSC). DSC heating scans of fibers electrospun from 20% nylon-6, 15% NC5 and 20% NC5 solutions are shown in Fig. 6. The electrospun nylon-6 fibers exhibited a melting point at 223.8 °C due to the melting of α-form of crystal (Fig. 6a). However, the electrospun nanocomposite fibers showed a slightly higher melting temperature around 225.0 °C (Fig. 6b and c). The higher melting point observed for the electrospun nanocomposite fibers indicated that the nylon-6 crystals were more perfect in the nanocomposite fibers. A small endothermic shoulder associated with melting of the γ-form of nylon-6 crystals [34] was observed in all heating scans at a temperature slightly lower than the main melting point (Fig. 6). In addition, a high temperature endotherm at about 238 °C resulting from the melting of a more stable crystal phase was observed only for electrospun NC5 fibers. This melting transition has also been reported for extruded nylon-6/MMT nanocomposites [34,35]. This more stable crystal phase consists of γ-form of crystals stabilized by the presence of silicate layers in the melt-extruded nylon-6/MMT composite [34]. The degree of crystallinity of nylon-6 and NC5 electrospun fibers measured by DSC was calculated from the ratio of $(\Delta H_f - \Delta H_c)$ to the heat of fusion of the purely crystalline forms of nylon-6 (ΔH_f^0), where ΔH_f and ΔH_c are the heat of fusion and heat of cold crystallization of electrospun fibrous mats, respectively [36]. Several different ΔH_f^0 values for the perfect nylon-6 crystal have been reported in the literature, such as 190 J/g [8,37–39], 230 J/g [36], and 240 J/g [6,34]. The ΔH_f^0 value of 240 J/g was used here to calculate the degree of crystallinity of nylon-6. The overall degree of crystallinity of nylon-6 obtained from DSC measurements was 9.1%, 18.1% and 17.0%, respectively, for the fibers electrospun from nylon-6, 15% NC5 and 20% NC5 solutions. Compared with the values from WAXD measurement (Table 2), the degree of nylon-6 crystallinity measured by DSC was higher due to the complexity to determine the cold crystallization peak of nylon-6 [36]. WAXD and DSC measurements showed that electrospun NC5 nanocomposite fibers had a higher degree of crystallinity than nylon-6 fibers. Nylon-6 crystals were also larger and more perfect in the NC5 electrospun fibers.

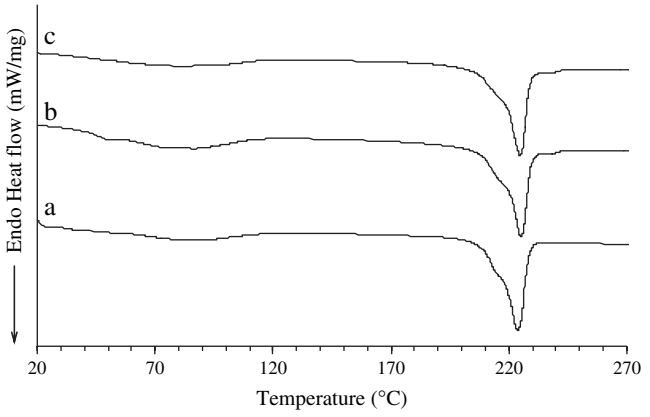

Fig. 6. DSC heating scans of (a) electrospun nylon-6 fibers; and nylon-6/O-MMT nanocomposite fibers electrospun from (b) 15% and (c) 20% NC5 solutions.

3.4. Mechanical properties

The average tensile modulus, ultimate tensile strength and ultimate strain derived from the tensile stress–strain curves for the electrospun mats are summarized in Table 3. When compared with the electrospun nylon-6 mats, the Young's modulus and ultimate strength of the nanocomposite mats electrospun from 15% NC5 solution were 70% and 30% larger, respectively. Although the fibrous mats electrospun from 20% NC5 solution exhibited a 43% increase in the Young's

Table 3
Tensile properties of electrospun nylon-6 and NC5 nanocomposite fibrous mats

Sample	Young's modulus (MPa)	Ultimate strength (MPa)	Ultimate strain (%)
Nylon-6	43.8 (3.5)[a]	6.8 (1.0)	25.7 (3.2)
15% NC5	76.0 (5.9)	8.9 (1.5)	17.6 (3.0)
20% NC5	62.6 (4.0)	5.3 (0.7)	18.5 (3.7)

[a] The values in the parentheses are the standard deviations of the measurements.

modulus, the ultimate tensile strength was lowered by about 20%. The ultimate strain of the NC5 mats electrospun from 15% and 20% NC5 solutions was decreased by about 28% (Table 3). These results correlated as expected with fibrous mats that comprised of more crystalline fibers (15% NC5 > 20% NC5 > nylon-6) exhibiting higher Young's modulus.

In addition to the individual fiber properties, the interaction between fibers in the fibrous mats contributed to the mechanical properties of the mats. The nanocomposite fibers electrospun from 15% NC5 solution exhibited the finest fiber sizes and many nanofibrils between the primary nanofibers (Figs. 2 and 4) provided more contacts and thus stronger cohesion among fibers. Therefore, the nanocomposite fibrous mats electrospun from the 15% NC5 solution were much stiffer and stronger than the electrospun nylon-6 fibrous mats. On the other hand, the much larger sizes of the fibers electrospun from the 20% NC5 solution (Fig. 2) resulted in decreased ultimate strength compared with the nylon-6 electrospun mats. Kwon et al. has observed that the electrospun poly(L-lactide-*co*-ε-caprolactone) (PLCL 50/50) mats composed of smaller fibers exhibited a higher Young's modulus due to the higher fiber packing density [24].

The Young's moduli of single electrospun nylon-6 and NC5 nanocomposite fibers were also measured and compared using an AFM. The individual electrospun fibers were suspended over the trenches on a silicon wafer (Fig. 7) and depressed at the center position by an AFM probe with a calibrated spring constant in contact mode. Only the fibers that were not contacted by others over the trench and not sagging into the trench, as confirmed by the AFM vision system, were used for the measurement. The raw AFM force curves were translated to force–displacement curves by converting the tip deflection to a force using the calibrated cantilever spring constant and converting the height of the AFM probe to fiber displacement [40]. A third-order polynomial equation for the displacement of a suspended elastic string with fix ends was used to calculate the Young's modulus (E) of the fiber. The lower order terms, which include terms due to initial tension in the fiber and the restoring force due to bending, were ignored, and the Young's modulus was extracted from the cubic term [27,41].

$$F = 8AE(\delta/L)^3$$

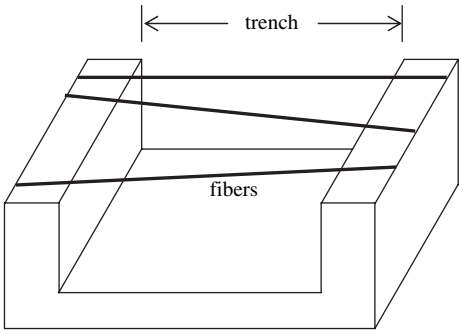

Fig. 7. Diagram of the deposition of three fibers across the trench.

where A is the cross-sectional area of the fiber, δ is the fiber displacement, and L is the suspended length of the fiber, which was calculated from the width of the trench measured by AFM and the angle of the fiber with respect to the trench walls was determined using the vision system of the AFM. In order to calculate the cross-sectional area, the fiber was assumed to have a circular cross-section and the height of the fiber above the wafer substrate measured by the AFM was used as the diameter. Since the nanocomposite fibers electrospun from the 20% NC5 solution mainly showed flat-sheet fiber morphology (Fig. 2c), only those electrospun from the 15% NC5 solution, which were confirmed to have a circular cross-section (Fig. 4), were used to measure the Young's modulus of single NC5 nanocomposite fibers. Fig. 8 shows an example of measured force curves for NC5 fibers, and the fit of the third-order polynomial model. The Young's modulus calculated from the cubic term of this particular force curve was 53 GPa. Several force curves were generated for each fiber to calculate the average Young's modulus. The sources of measurement errors for the different fibers include variation in fiber cross-sectional area, inaccuracies in the measured suspended fiber length, and any difference between the center of the trench and the point of contact between AFM tip and the fiber [27]. Fig. 9 shows that the Young's moduli of the electrospun nylon-6 and NC5 nanocomposite fibers increased with decreasing fiber diameters. Smaller electrospun nanofibers are known to have fewer structural imperfections, such as the unavoidable chain ends, and a higher degree of molecular chain orientation along the fiber axis due to the higher stress experienced by the smaller fibers during the electrospinning [11], both of which could result in higher Young's modulus of the smaller electrospun fibers [42].

The highest Young's modulus obtained for the electrospun nylon-6 single fiber was about 30 GPa (Fig. 9), which was much larger than the highest value that had been achieved for conventional nylon-6 fibers, 15 GPa, but still significantly

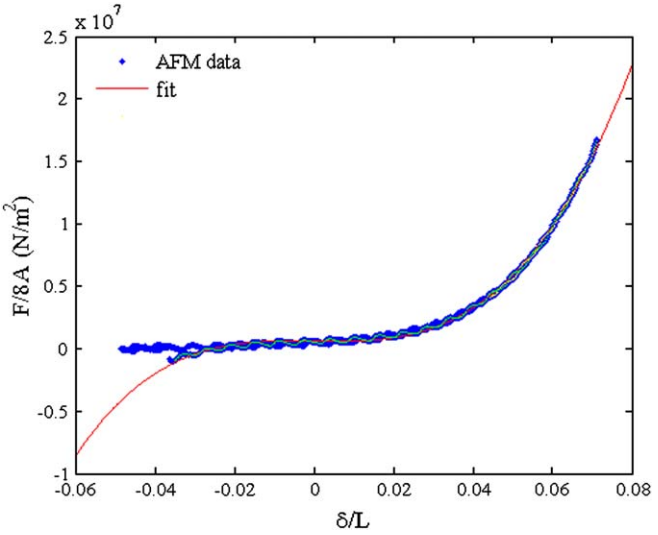

Fig. 8. Typical force–displacement curve for a suspended nylon-6/O-MMT nanocomposite fiber. The displacement is arbitrarily set to zero at the contact point. The slight oscillation in the signal is an artifact produced by the AFM due to the changes in the optical path length traveled by the laser.

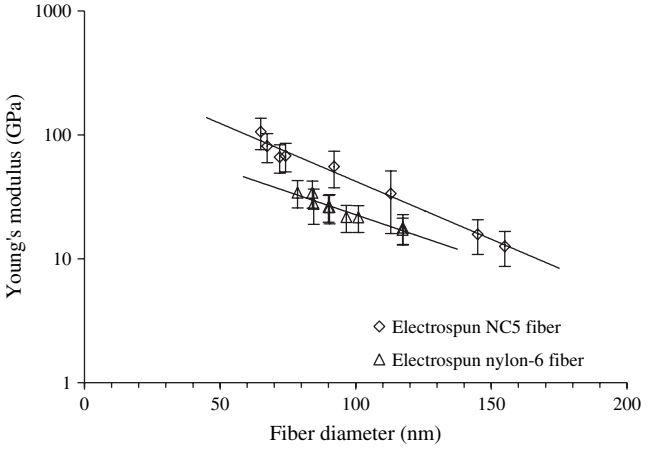

Fig. 9. Average Young's modulus of electrospun nylon-6 and nylon-6/O-MMT nanocomposite single fibers versus the fiber diameter.

lower than the Young's modulus, 174 GPa, measured by X-ray diffraction from nylon-6 crystals stressed in the chain axis direction [42] or the calculated theoretical limit of Young's modulus along the chain direction for the α-form of nylon-6, 312 GPa [42,43]. Fig. 9 shows that the Young's moduli of electrospun NC5 single fibers were improved by about 100% when compared with electrospun nylon-6 single fibers of similar fiber diameters. The increase in the Young's modulus of individual fibers was greater than the improvement observed for the electrospun fibrous mats, 70%.

4. Conclusions

Nylon-6 fibers and NC5 nanocomposite fibers with average diameters around 100 nm were successfully prepared by electrospinning using 88% aqueous formic acid as the solvent. The addition of O-MMT layers in the nylon-6 solution increased the solution viscosity significantly and changed the resulting fiber morphology and sizes.

TEM images of NC5 nanocomposite fibers and ultra-thin fiber sections and the WAXD results showed that O-MMT layers were well exfoliated inside the nanocomposite fibers and oriented along the fiber axial direction. The degree of crystallinity and crystallite size were both increased for the nanocomposite fibers and more significant for the fibers electrospun from 15% NC5 solution, which exhibited the finest average fiber size. As a result, the tensile properties of electrospun NC5 were greatly improved. The Young's modulus and ultimate strength of electrospun nanocomposite fibrous mats were improved up to 70% and 30%, respectively, when compared with nylon-6 electrospun mats. However, the ultimate strength of the nanocomposite fibrous mats electrospun from 20% NC5 solution was decreased by about 20% due to their larger fiber sizes. The Young's modulus of nylon-6 electrospun single fibers with a diameter around 80 nm was almost double the highest value that had been reported for the conventional nylon-6 fibers and could be improved by about 100% for the electrospun NC5 nanocomposite single fibers of similar diameters. The electrospun NC5 nanocomposite fibers have great potential for the applications where both high surface-to-volume ratio and strong mechanical properties are required such as the high-performance filters and fiber reinforcement materials.

Acknowledgement

The authors thank Tom B. Green for helpful discussion and United Air Specialists Inc., Clark Filter, and CLARCOR Inc. for financial support. This work made use of the Cornell Center for Materials Research Facilities supported by the National Science Foundation under Award Number DMR-0520404. The silicon processing was done at the Cornell Nano-Scale Science & Technology Facility (a member of the National Nanofabrication Users Network) which is supported by the National Science Foundation under Grant ECS-9731293. This material is based upon work supported in part by the STC Program of the National Science Foundation under Agreement No. ECS-9876771.

References

[1] Giannelis EP. Applied Organometallic Chemistry 1998;12(10–11):675–80.
[2] Cho JW, Paul DR. Polymer 2001;42(3):1083–94.
[3] Giannelis EP. Advanced Materials 1996;8(1):29.
[4] Yano K, Usuki A, Okada A, Kurauchi T, Kamigaito O. Journal of Polymer Science, Part A: Polymer Chemistry 1993;31(10):2493–8.
[5] Lincoln DM, Vaia RA, Wang ZG, Hsiao BS. Polymer 2001;42(4):1621–31.
[6] Fornes TD, Paul DR. Polymer 2003;44(14):3945–61.
[7] Vaia RA, Jandt KD, Kramer EJ, Giannelis EP. Chemistry of Materials 1996;8(11):2628–35.
[8] Fong H, Liu W, Wang C-S, Vaia RA. Polymer 2001;43(3):775–80.
[9] Hong JH, Jeong EH, Lee HS, Baik DH, Seo SW, Youk JH. Journal of Polymer Science, Part B: Polymer Physics 2005;43(22):3171–7.
[10] Wang M, Hsieh AJ, Rutledge GC. Polymer 2005;46(10):3407–18.
[11] Ji Y, Li BQ, Ge SR, Sokolov JC, Rafailovich MH. Langmuir 2006;22(3):1321–8.
[12] Zhou H, Kim K-W, Giannelis EP, Joo YL. Nanofibers from poly(lactic) acid nanocomposites. In: Reneker DH, Fong H, editors. Polymeric nanofibers. Washington, D.C.: American Chemical Society: Distributed by Oxford University Press; 2006. p. 217–30.
[13] Dzenis Y. Science 2004;304(5679):1917–9.
[14] Reneker DH, Chun I. Nanotechnology 1996;7(3):216–23.
[15] Doshi J, Reneker DH. Journal of Electrostatics 1995;35(2&3):151–60.
[16] Reneker DH. In: Proceedings – world filtration congress, 9th, New Orleans, LA, United States, April 18–24, 2004; 2004. p. 1802–9.
[17] Li L, Green TB, Frey MW. Journal of Engineered Fibers and Fabrics, in press.
[18] Bowlin GL, Simpson DG, Wnek G. Electroprocessing polymers to form footwear and clothing. In: U.S. Pat Appl Publ (USA). US 2003207638; 2003, p. 24, Cont.-in-part of U.S. Ser. No. 714, 255.
[19] Bergshoef MM, Vancso GJ. Advanced Materials (Weinheim, Germany) 1999;11(16):1362–5.
[20] Li L, Hsieh Y-L. Nanotechnology 2005;16(12):2852–60.
[21] Kenawy El R, Layman John M, Watkins Jessica R, Bowlin Gary L, Matthews Jamil A, Simpson David G, et al. Biomaterials 2003;24(6):907–13.
[22] Ko F, Gogotsi Y, Ali A, Naguib N, Ye HH, Yang GL, et al. Advanced Materials 2003;15(14):1161.
[23] Hou HQ, Ge JJ, Zeng J, Li Q, Reneker DH, Greiner A, et al. Chemistry of Materials 2005;17(5):967–73.
[24] Kwon IK, Kidoaki S, Matsuda T. Biomaterials 2005;26(18):3929–39.
[25] Kim GM, Lach R, Michler GH, Chang YW. Macromolecular Rapid Communications 2005;26(9):728–33.

[26] Wang M, Jin H-J, Kaplan DL, Rutledge GC. Macromolecules 2004;37(18):6856–64.
[27] Bellan LM, Kameoka J, Craighead HG. Nanotechnology 2005;16(8): 1095–9.
[28] Nicholson ED, Baker TW, Redman SA, Kalaugher E, Rosser KN, Everitt NM, et al. Diamond and Related Materials 1996;5(6–8): 658–63.
[29] Klug T, Reichert J, Bruckner R. Journal of Materials Science 1993;28(23):6303–6.
[30] Dennis HR, Hunter DL, Chang D, Kim S, White JL, Cho JW, et al. Polymer 2001;42(23):9513–22.
[31] Fornes TD, Yoon PJ, Keskkula H, Paul DR. Polymer 2001;42(25): 9929–40.
[32] Koombhongse S, Liu W, Reneker DH. Journal of Polymer Science, Part B: Polymer Physics 2001;39(21):2598–606.
[33] Zhao ZD, Yu WX, Liu YH, Zhang JQ, Shao ZJ. Materials Letters 2004;58(5):802–6.
[34] Winberg P, Eldrup M, Pedersen NJ, van Es MA, Maurer FHJ. Polymer 2005;46(19):8239–49.
[35] Medellin-Rodriguez FJ, Burger C, Hsiao BS, Chu B, Vaia R, Phillips S. Polymer 2001;42(21):9015–23.
[36] Khanna YP, Kuhn WP. Journal of Polymer Science, Part B: Polymer Physics 1997;35(14):2219–31.
[37] Xie S, Zhang S, Liu H, Chen G, Feng M, Qin H, et al. Polymer 2005;46(14):5417–27.
[38] Wu QJ, Liu XH, Berglund LA. Macromolecular Rapid Communications 2001;22(17):1438–40.
[39] Campoy I, Gomez MA, Marco C. Polymer 1998;39(25):6279–88.
[40] Tombler TW, Zhou CW, Alexseyev L, Kong J, Dai HJ, Lei L, et al. Nature 2000;405(6788):769–72.
[41] Timoshenko S. Strength of materials. 2nd ed. New York: Van Nostrand-Reinhold; 1940. p. 2v.
[42] Crist B. Annual Review of Materials Science 1995;25:295–323.
[43] Tashiro K, Tadokoro H. Macromolecules 1981;14(3):781–5.